Self-organized criticality and Tropical Geometry

Ernesto Lupercio (Cinvestav - México)
(joint with: N. Kalinin, A. Guzman-Saenz, Y. Prieto, M. Shkolnikov, and V. Kalinina, and also Ramiro Hum-Sah López Vázquez)

September 7, 2019

First Part: Self-Organized Criticality

Figure: *La trahison des images*, 1928, René Magritte

The naturals under addition

Figure: *Ce n'est pas des mathématiques.* A super-computer

CV by Leonardo (30 years old)

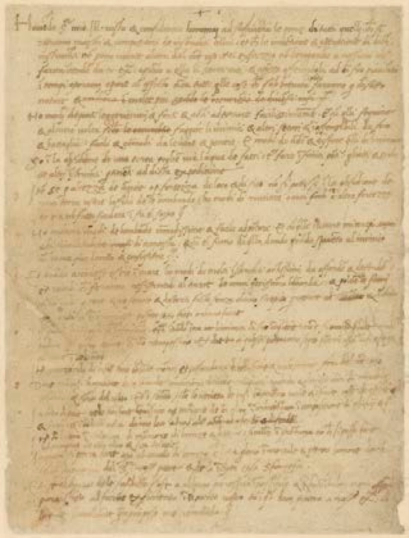

Figure: “and in paiting I am as good as anyone”

Los cuadernos de Leonardo

Figure: “all branches of the tree, in each of their developments, together equal the thickness of the tree”

Las citas de Leonardo

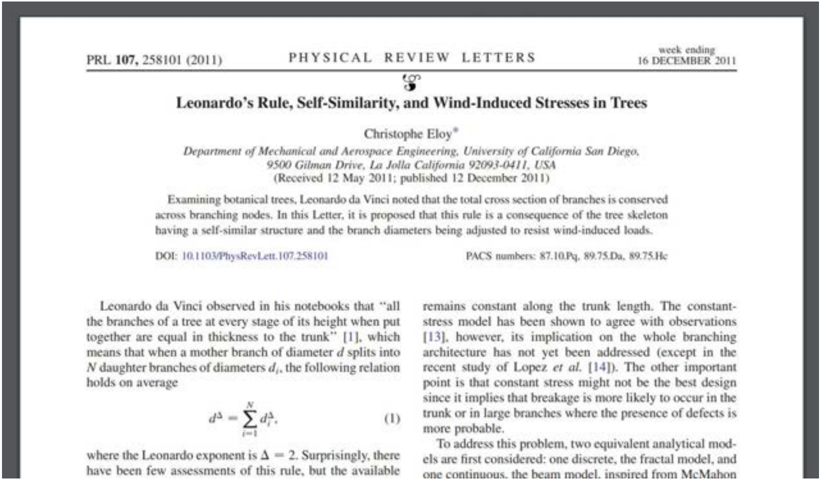

PRL 107, 258101 (2011) PHYSICAL REVIEW LETTERS week ending 16 DECEMBER 2011

Leonardo's Rule, Self-Similarity, and Wind-Induced Stresses in Trees

Christophe Eloy*
Department of Mechanical and Aerospace Engineering, University of California San Diego, 9500 Gilman Drive, La Jolla California 92093-0411, USA
(Received 12 May 2011; published 12 December 2011)

Examining botanical trees, Leonardo da Vinci noted that the total cross section of branches is conserved across branching nodes. In this Letter, it is proposed that this rule is a consequence of the tree skeleton having a self-similar structure and the branch diameters being adjusted to resist wind-induced loads.

DOI: 10.1103/PhysRevLett.107.258101 PACS numbers: 87.10.Pq, 89.75.Da, 89.75.Hc

Leonardo da Vinci observed in his notebooks that "all the branches of a tree at every stage of its height when put together are equal in thickness to the trunk" [1], which means that when a mother branch of diameter d splits into N daughter branches of diameters d_i, the following relation holds on average

$$d^{\Delta} = \sum_{i=1}^{N} d_i^{\Delta}, \quad (1)$$

where the Leonardo exponent is $\Delta = 2$. Surprisingly, there have been few assessments of this rule, but the available

remains constant along the trunk length. The constant-stress model has been shown to agree with observations [13], however, its implication on the whole branching architecture has not yet been addressed (except in the recent study of Lopez *et al.* [14]). The other important point is that constant stress might not be the best design since it implies that breakage is more likely to occur in the trunk or in large branches where the presence of defects is more probable.

To address this problem, two equivalent analytical models are first considered: one discrete, the fractal model, and one continuous, the beam model, inspired from McMahon

Figure: Physical Review Letters, 2011

Las citas de Leonardo

OPEN ACCESS Freely available online

PLOS | ONE

Tree Branching: Leonardo da Vinci's Rule versus Biomechanical Models

Ryoko Minamino*, Masaki Tateno

Nikko Botanical Garden, Graduate School of Science, The University of Tokyo, Nikko, Tochigi, Japan

Abstract

This study examined Leonardo da Vinci's rule (*i.e.*, the sum of the cross-sectional area of all tree branches above a branching point at any height is equal to the cross-sectional area of the trunk or the branch immediately below the branching point) using simulations based on two biomechanical models: the uniform stress and elastic similarity models. Model calculations of the daughter/mother ratio (*i.e.*, the ratio of the total cross-sectional area of the daughter branches to the cross-sectional area of the mother branch at the branching point) showed that both biomechanical models agreed with da Vinci's rule when the branching angles of daughter branches and the weights of lateral daughter branches were small; however, the models deviated from da Vinci's rule as the weights and/or the branching angles of lateral daughter branches increased. The calculated values of the two models were largely similar but differed in some ways. Field measurements of *Fagus crenata* and *Abies homolepis* also fit this trend, wherein models deviated from da Vinci's rule with increasing relative weights of lateral daughter branches. However, this deviation was small for a branching pattern in nature, where empirical measurements were taken under realistic measurement conditions; thus, da Vinci's rule did not critically contradict the biomechanical models in the case of real branching patterns, though the model calculations described the contradiction between da Vinci's rule and the biomechanical models. The field data for *Fagus crenata* fit the uniform stress model best, indicating that stress uniformity is the key constraint of branch morphology in *Fagus crenata* rather than elastic similarity or da Vinci's rule. On the other hand, mechanical constraints are not necessarily significant in the morphology of *Abies homolepis* branches, depending on the number of daughter branches. Rather, these branches were often in agreement with da Vinci's rule.

Citation: Minamino R, Tateno M (2014) Tree Branching: Leonardo da Vinci's Rule versus Biomechanical Models. PLoS ONE 9(4): e93535. doi:10.1371/journal.pone.0093535

Figure: PLOS One, 2014

The Sandpile Cellular Automaton

Figure: Xiuhcoatl, the super-computer

Zipf's Law (from G. West, Scale)

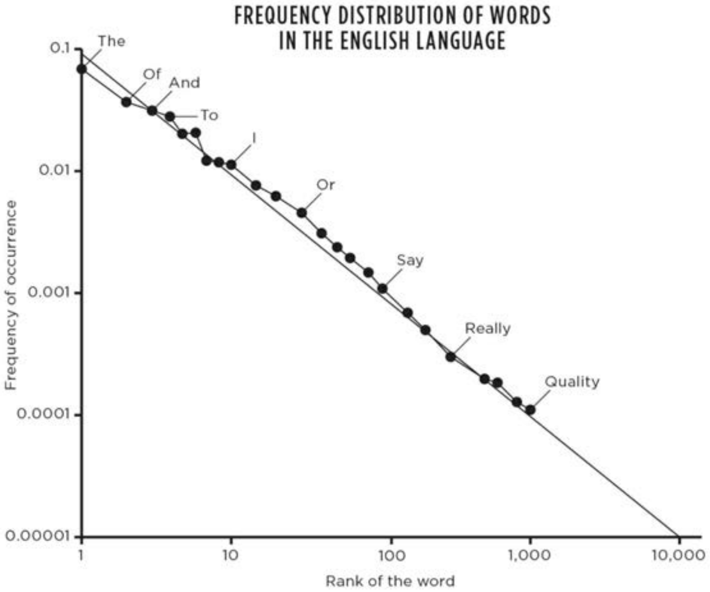

Body Weight

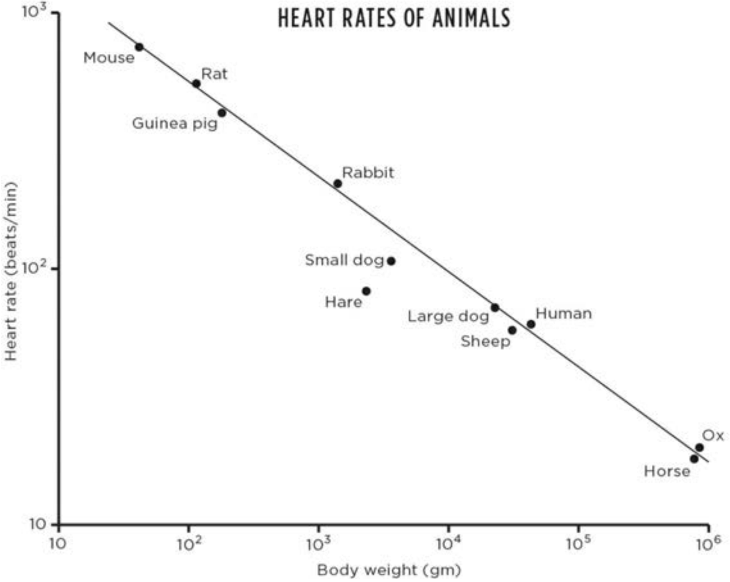
HEART RATES OF ANIMALS
Mouse
Rat
Guinea pig
Rabbit
Small dog
Hare
Large dog
Sheep
Human
Ox
Horse
Heart rate (beats/min)
Body weight (gm)
10
10^2
10^3
10^4
10^5
10^6

Metabolism

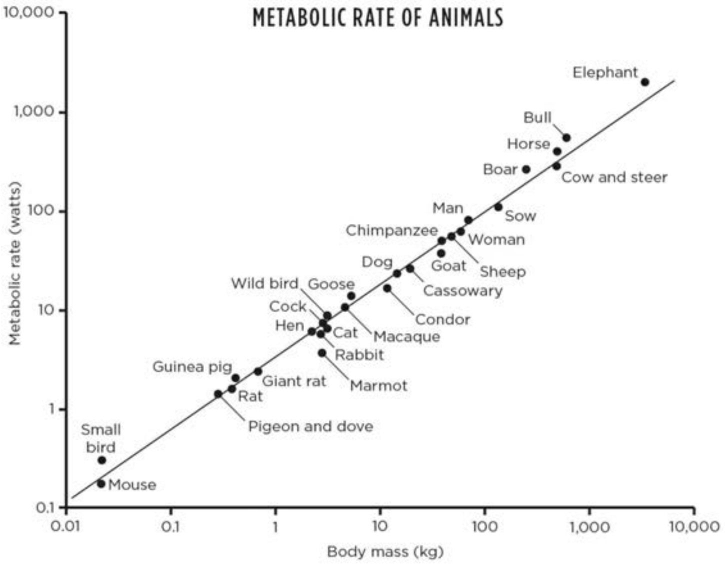
METABOLIC RATE OF ANIMALS
Metabolic rate (watts)
10,000
1,000
100
10
1
0.1
Body mass (kg)
0.01
0.1
1
10
100
1,000
10,000
Elephant
Bull
Horse
Boar
Cow and steer
Man
Sow
Chimpanzee
Woman
Dog
Goat
Sheep
Cassowary
Wild bird
Goose
Cock
Hen
Cat
Macaque
Condor
Rabbit
Marmot
Guinea pig
Giant rat
Rat
Pigeon and dove
Small bird
Mouse

Earthquake frecuency by size

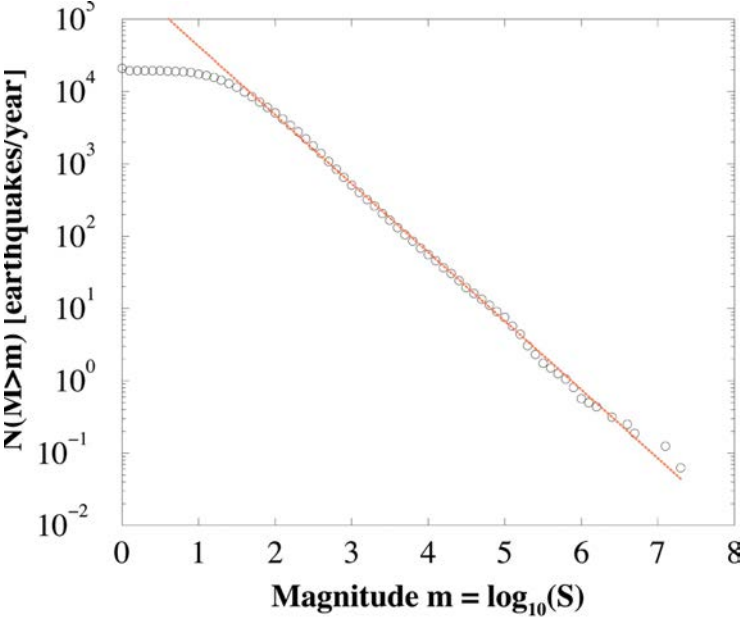

Earthquake frecuency by size and region

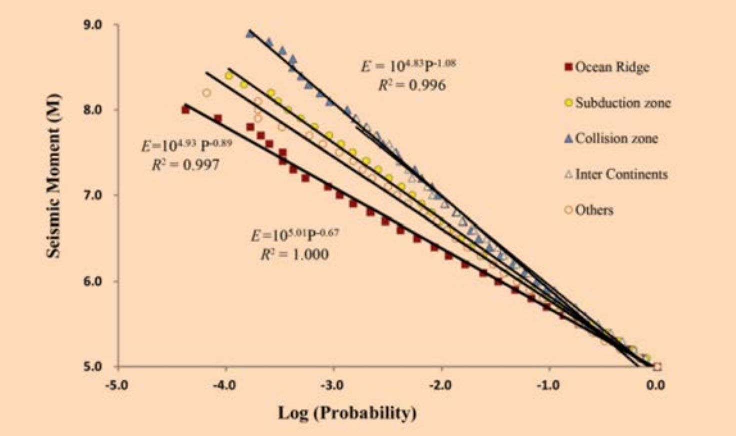

Figure: Power Law

The Sandpile Cellular Automaton

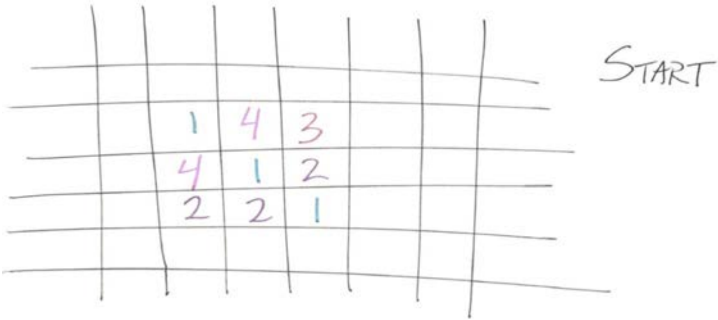

Figure: Intermediate State

The Sandpile Cellular Automaton

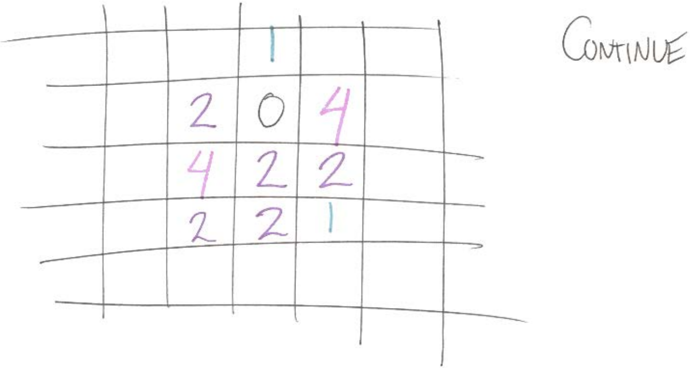

Figure: Intermediate State

The Sandpile Cellular Automaton

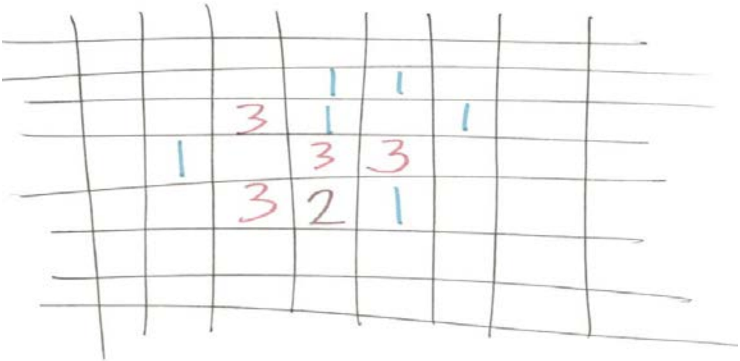

Figure: The unique final state

The Sandpile Cellular Automaton

Figure: A very large table

The Sandpile Cellular Automaton

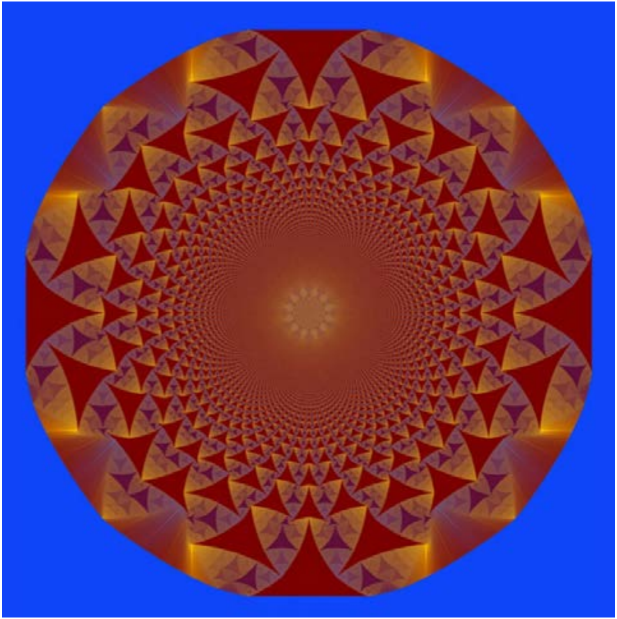

Self-Organized Criticality

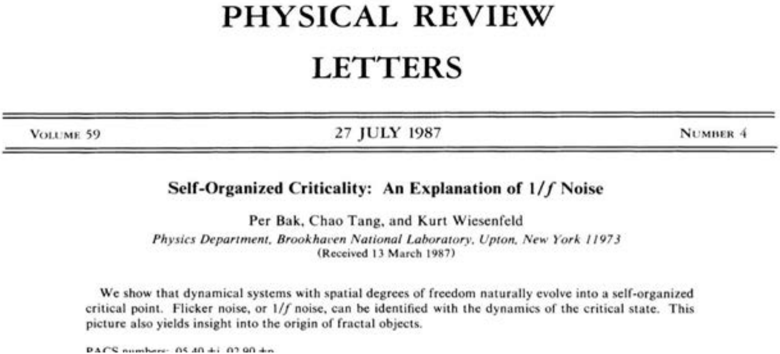

PHYSICAL REVIEW LETTERS

VOLUME 59 27 JULY 1987 NUMBER 4

Self-Organized Criticality: An Explanation of 1/*f* Noise

Per Bak, Chao Tang, and Kurt Wiesenfeld

Physics Department, Brookhaven National Laboratory, Upton, New York 11973

(Received 13 March 1987)

We show that dynamical systems with spatial degrees of freedom naturally evolve into a self-organized critical point. Flicker noise, or 1/*f* noise, can be identified with the dynamics of the critical state. This picture also yields insight into the origin of fractal objects.

PACS numbers: 05.40.+j, 02.90.+p

Figure: The most cited paper in Physics in the 90's

Self-Organized Criticality

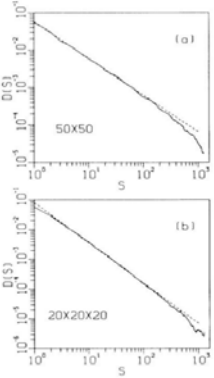

FIG. 2. Distribution of cluster sizes at criticality in two and three dimensions, computed dynamically as described in the text. (a) 50×50 array, averaged over 200 samples; (b) $20\times 20\times 20$ array, averaged over 200 samples. The data have been coarse grained.

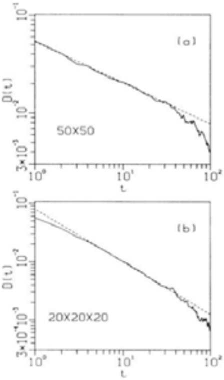

FIG. 3. Distribution of lifetimes corresponding to Fig. 2. (a) For the 50×50 array, the slope $\alpha \approx 0.42$, yielding a "$1/f$" noise spectrum $f^{-1.58}$; (b) $20\times 20\times 20$ array, $\alpha \approx 0.90$, yielding an $f^{-1.1}$ spectrum

Figure: The original computer calculations.

Real Sand

SOC Timeline

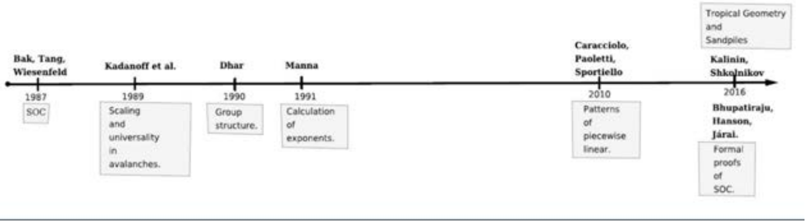

The Sandpile Cellular Automaton

Brains May Teeter Near Their Tipping Point

In a renewed attempt at a grand unified theory of brain function, physicists now argue that brains optimize performance by staying near — though not exactly at — the critical point between two phases.

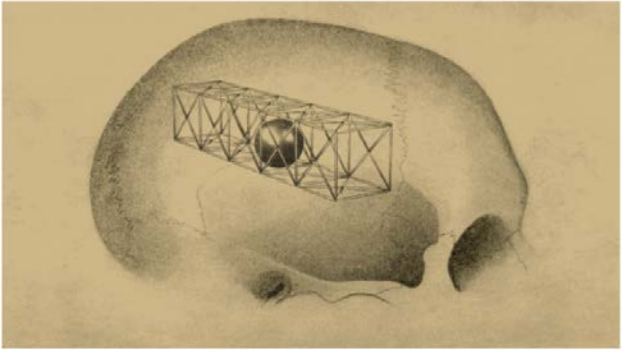

Bill Domonkos for Quanta Magazine

Figure: Is the brain in SOC?

First relation to geometry

- This can be generalized to any graph G (finite, with a sink).
- The configuration space of this discrete dynamical system is meant to be though of as the space of divisors of a graph (or tropical curve).
- There is the subgroup of stable configurations,
- and the subgroup of recurrent configurations (a stable configuration is recurrent if it can be obtained from any other configuration by adding chips and stabilizing.) Think probability one in the Markov chain.

First relation to geometry

- The **sandpile group** is the set of recurrent configurations.
- This is the same as the "tropical jacobian" of the "tropical curve" $J(G)$.
- It has as many elements as spanning trees has G, that is to say, te determinan of the "tropical laplacian" (matrix tree theorem).
- But this relaiton to geometry is NOT what we mean to discuss today.

Zoom in

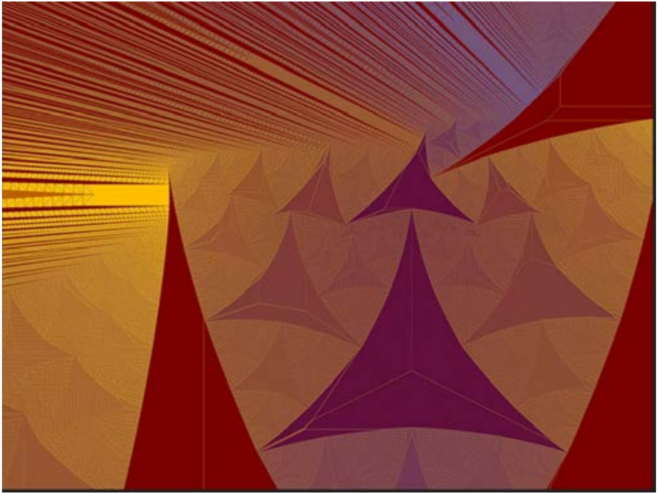

Figure: Notice the thin graphs inside the triangles

Rescaling

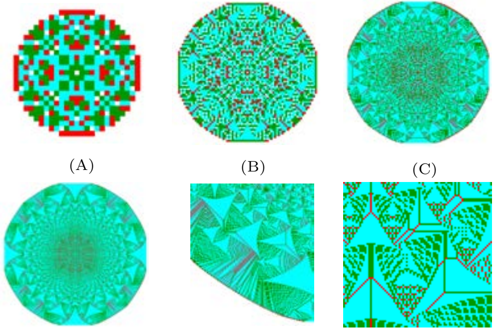

(A) (B) (C)

(D) (E) (F)

Fig. 2. In (A), (B), (C) and (D), a very large number N of grains of sand is placed at the origin of the everywhere empty integral lattice, the final relaxed state shows fractal behavior. Here, as we advance from (A) to (D), we see successive sandpiles for $N = 10^3$ (A), 10^4 (B), 10^5 (C), and 10^6 (D), rescaled by factors of $\sqrt{N}$. In (E), we zoom in on a small region of (D) to show its intricate fractal structure, and, finally, in (F), we further zoom in on a small portion of (E). We can see proportional growth occurring in the patterns as the fractal limit appears. The balanced graphs inside the roughly triangular regions of (F) are tropical curves.

Figure: Notice the thin graphs inside the triangles

The Laplacian

- The *toppling function* $H(i,j)$ defined as follows: Given an initial state ϕ and its relaxation φ°, the value of $H(i,j)$ equals the number of times that there was a toppling at the vertex (i,j) in the process taking φ to φ°.
- The discrete Laplacian of H is defined by the net flow of sand,

$$\Delta H(i,j) := H(i-1,j) + H(i+1,j) + H(i,j-1) + H(i,j+1) - 4H(i,j).$$

The Laplacian determines the evolution

The toppling function is clearly non-negative on Ω and vanishes at the boundary. The function ΔH completely determines the final state φ° by the formula:

$$\varphi^\circ(i,j) = \varphi(i,j) + \Delta H(i,j). \tag{1}$$

The Least Action Principle

It can be shown by induction that the toppling function H satisfies the *Least Action Principle*: if $\varphi(i,j) + \Delta F(i,j) \leq 3$ is stable, then $F(i,j) \geq H(i,j)$. Ostojic noticed that $H(i,j)$ is a piecewise quadratic function in the usual sandpile.

Tropical Sandpiles

Consider a state φ which consists of 3 grains of sand at every vertex, except at a finite family of points

$$P = \{p_1 = (i_1, j_1), \ldots, p_r = (i_r, j_r)\}$$

where we have 4 grains of sand:

$$\varphi := \langle 3 \rangle + \delta_{p_1} + \cdots + \delta_{p_r} = \langle 3 \rangle + \delta_P. \qquad (2)$$

The state φ° and the evolution of the relaxation can be described by means of tropical geometry. This was discovered by Caracciolo et al. while a rigorous mathematical theory to prove this fact has been given by Kalinin and Shkolnikov.
It is a remarkable fact that, in this case, the toppling function $H(i,j)$ is piecewise linear (after passing to the scaling limit).

A Tropical Sandpile (Kalinin-Shkolnikov)

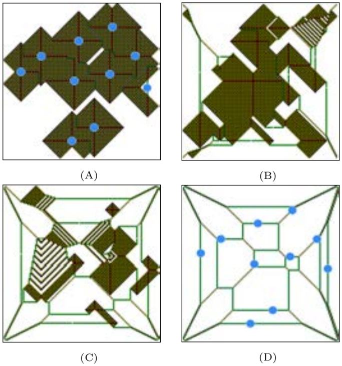

Fig. 4. The evolution of $\langle 3 \rangle + \delta_P$. Sand falling outside the border disappears. Time progresses in the sequence (A), (B), (C), and finally (D). Before (A), we add grains of sand to several points of the constant state $\langle 3 \rangle$ (we see their positions as blue disks given by δ_P). Avalanches ensue. At time (A), the avalanches have barely started. At the end, at time (D), we get a tropical analytic curve on the square Ω. White represents the region with 3 grains of sand while green represent 2, yellow represents 1, and red represents the zero region. We can think of the blue disks δ_P as the genotype of the system, of the state $\langle 3 \rangle$ as the nutrient environment, and of the thin graph given by the tropical function in (D) as the phenotype of the system.

Figure: Time advances from left to right

A Tropical Sandpile

A movie:

Idea of the Proof (1)

To prove this, one considers the family $\mathcal{F}_P$ of functions on Ω that are:

1. (1) piecewise linear with integral slopes,
2. (2) non-negative over Ω and zero at its boundary,
3. (3) concave, and
4. (4) not smooth at every point p_i of P.

Let F_P be the pointwise minimum of functions in $\mathcal{F}_P$. Then $F_P \geq H$ by the Least Action Principle.

Idea of the Proof (2)

Lemma

In the scaling limit $H = F_P$.

A sketch of a proof. K-S introduce the wave operators W_p at the cellular automaton level and the corresponding tropical wave operators G_p. Given a fixed vertex $p = (i_0, j_0)$, we define the wave operator W_p acting on states φ of the sandpile as:

$$W_p(\varphi) := (T_p(\varphi + \delta_p) - \delta_p)^\circ,$$

where T_p is the operator that topples once the state $\varphi + \delta_p$ at p if at all possible. In a computer simulation, the application of this operator looks like a wave of topplings spreading from p, while each vertex topples at most once.

The wave operator (1)

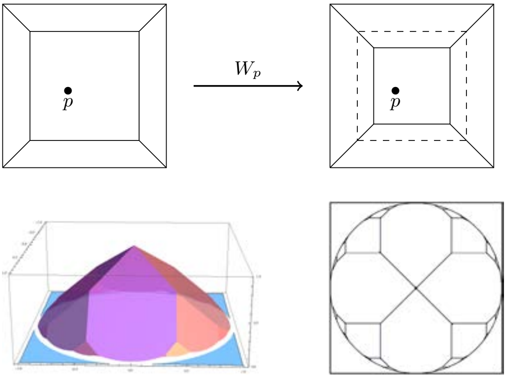

Fig. 5. Top: The action of the wave operator W_p on a tropical curve. The tropical curve steps closer to p by an integral step. Thus W_p shrinks the face that p belongs to; the combinatorial morphology of the face that p belongs to, can actually change. Bottom: The function $G_p\mathbf{0}$, where p is the center of the circle, and its associated omega-tropical curve are shown.

The wave operator (2)

The first important property of W_p is that, for the initial state $\varphi := \langle 3 \rangle + \delta_P$, we can achieve the final state φ° by successive applications of the operator $W_{p_1} \circ \cdots \circ W_{p_r}$ a large but finite number of times (in spite of the notation):

$$\varphi^\circ = (W_{p_1} \cdots W_{p_r})^\infty \varphi + \delta_P.$$

This process decomposes the total relaxation $\varphi \mapsto \varphi^\circ$ into layers of controlled avalanching.

The wave operator (3)

The second important property of the wave operator W_p is that its action on a state $\varphi = \langle 3 \rangle + \Delta f$ has an interpretation in terms of tropical geometry. To wit, whenever f is a piecewise linear function with integral slopes that, in a neighborhood of p, is expressed as $a_{i_0 j_0} + i_0 x + j_0 y$, we have that

$$W_p(\langle 3 \rangle + \Delta f) = \langle 3 \rangle + \Delta W(f),$$

where $W(f)$ has the same coefficients a_{ij} as f except one, namely $a'_{i_0 j_0} = a_{i_0 j_0} + 1$. This is to emulate the fact that the support of the wave is exactly the face where $a_{i_0 j_0} + i_0 x + j_0 y$ is the leading part of f.

The dynamical system

- We will write $G_p := W_p^\infty$ to denote the operator that applies W_p to $\langle 3 \rangle + \Delta f$ until p lies in the corner locus of f.
- It has an elegant interpretation in terms of tropical geometry: G_p increases the coefficient $a_{i_0 j_0}$ corresponding to a neighborhood of p lifting the plane lying above p in the graph of f by integral steps until p belongs to the corner locus of $G_p f$. Thus G_p has the effect of pushing the tropical curve closer towards p until it contains p.

End of the Proof

From the properties of the wave operators, it follows immediately that:

$$F_P = (G_{p_1} \cdots G_{p_r})^{\infty}\,\mathbf{0},$$

where $\mathbf{0}$ is the function which is identically zero on Ω.

Each intermediate function $(G_{p_1} \cdots G_{p_r})^{k}\,\mathbf{0}$ is less than H since they represent partial relaxations, but their limit belongs to $\mathcal{F}_P$, and this, in turn, implies that $H = F_P$.

The Tropical Sandpile model (KGPSKL) (1)

Now, we define a new model, tropical sandpile (TS), reflecting structural changes when a sandpile evolves. The definition of this dynamical system is inspired by the mathematics of the previous section, and TS is not a cellular automaton but it exhibits SOC.

The Tropical Sandpile model (2)

The dynamical system lives on the convex set $\Omega = [0, N] \times [0, N]$; namely, we will consider Ω to be a very large square. The input data of the system is a large but finite collection of points $P = \{p_1, \dots, p_r\}$ with integer coordinates on the square Ω. Each state of the system is an Ω-tropical series (and the associated Ω-tropical curve).

Tropical Series

Definition

An Ω-tropical series is a piecewise linear function in Ω given by:

$$F(x, y) = \min_{(i,j)\in\mathcal{A}} (a_{ij} + ix + jy),$$

where the set $\mathcal{A}$ is not necessarily finite and $F|_{\partial\Omega} = 0$. An Ω-tropical curve is the set where F is not smooth. Each Ω-tropical curve is a locally finite graph satisfying the balancing condition.

The Tropical Sandpile model (3)

The initial state for the dynamical system is $F_0 = \mathbf{0}$, and its final state is the function F_P defined previously. Notice that the definition of $\mathcal{F}_P$, while inspired by sandpile theory, uses no sandpiles or cellular automaton whatsoever. Intermediate states $\{F_k\}_{k=1,\dots,r}$ enjoy the property that F_k is not smooth at $p_1, p_2, \dots, p_k$, i.e. the corresponding tropical curve passes through these points.

The Tropical Sandpile model (4)

In other words, the tropical curve is first attracted to the point p_1. Once it manages to pass through p_1 for the first time, it continues to try to pass through $\{p_1, p_2\}$. Once it manages to pass through $\{p_1, p_2\}$, it proceeds in the same manner towards $\{p_1, p_2, p_3\}$. The same process is repeated until the curve passes through all of $P = \{p_1, \ldots, p_r\}$.

The Tropical Sandpile model (5)

$\Omega = [0, 100] \times [0, 100]$

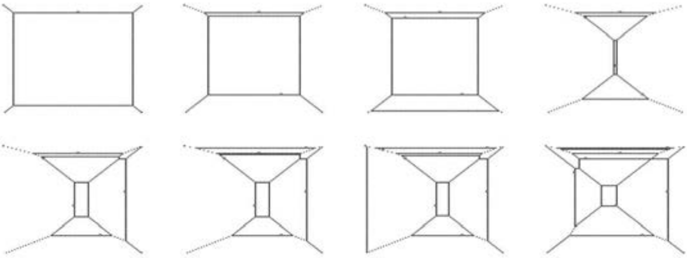

The Tropical Sandpile model (6)

We will call the modification $F_{k-1} \to F_k$ the k-th avalanche and it occurs as follows: To the state F_{k-1}, we apply the tropical operators $G_{p_1}, G_{p_2}, \ldots, G_{p_k}; G_{p_1}, \ldots$ in cyclic order until the function stops changing; the discreteness of the coordinates of the points in P ensures that this process is finite[1]. Again, as before, while sandpile inspired, the operators G_p are defined entirely in terms of tropical geometry without a mention to sandpiles.

There is a dichotomy: Each application of a G_p either does something changing the shape of the current tropical curve (in this case G_p is called an active operator), or does nothing, leaving the curve intact (if p already belongs to the curve).

[1] If the coordinates of the points in P are not integers, the model is well-defined, but we need to take a limit which is not suitable for computer simulations.

The Tropical Sandpile model (7)

Definition

The size of the k-th avalanche is the number of distinct active operators G_{p_i} (that actually do something) used to take the system from the self-critical state F_{k-1} to the next self-critical state F_k, divided by k. In particular, the size s_k of the k-th avalanche is a number between zero and one: $0 \leq s_k \leq 1$, and it estimates the proportional area of the picture which changed during the avalanche.

Spatial SOC

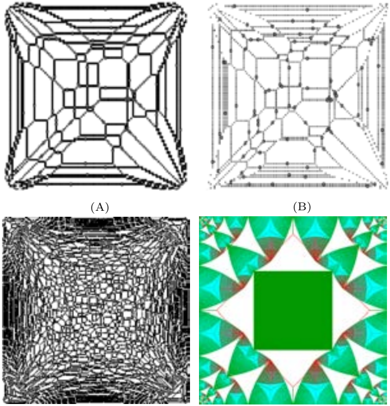

(A) (B) (C) (D)

Fig. 6. The first two pictures show the comparison between the classical (A) and tropical (B) sandpiles for $|P| = 100$ generic points on the square. In (C), the square Ω has side $N = 1000$; a large number ($|P| = 40000$) of grains has been added, showing the spatial SOC behavior on the tropical model compared to the identity (D) of the sandpile group on the square of side $N = 1000$. In the central square region on (C) (corresponding to the solid block of the otherwise fractal unit), we have a random tropical curve with edges on the directions $(1, 0)$, $(0, 1)$, and $(\pm 1, 1)$, which is given by a small perturbation of the coefficients of the tropical polynomial defining the usual square grid.

The Tropical Sandpile model (8)

In the previous example, as the number of points in P grows and becomes comparable to the number of lattice points in Ω, the tropical sandpile exhibits a phase transition going into spatial SOC (fractality). This provides the first evidence in favor of SOC on the tropical sandpile model, but there is a more subtle spatio-temporal SOC behavior that we proceed to exhibit in the following slides.

While the ordering of the points from the first to the r-th is important for the specific details of the evolution of the system, its statistical behavior and the final state are insensitive to it. This we called the Abelian property.

SOC in tropical geometry

The tropical sandpile dynamics exhibits slow driving avalanching.

Once the tropical dynamical system stops after r steps, we can ask ourselves what the statistical behavior of the number $N(s)$ of avalanches of size s is like. We posit that the tropical dynamical system exhibits spatio-temporal SOC behavior, namely, we have a power law:

$$\log N(s) = \tau \log s + c.$$

To confirm this, we have performed experiments in the supercomputing clusters ABACUS and Xiuhcoatl at Cinvestav (Mexico City); the code is available on GitHub. In the figure below, we see the graph of $\log N(s)$ vs $\log s$ for the tropical (piecewise linear, continuous) sandpile dynamical system, the resulting experimental τ in this case was $\tau \sim -0.9$.

SOC in tropical geometry

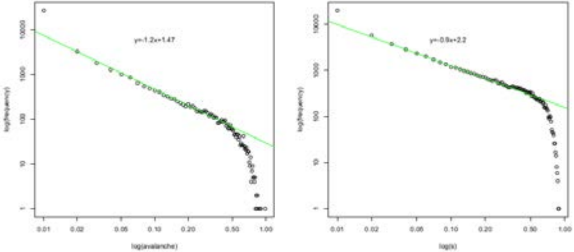

(A) Sandpile dynamical system

(B) Tropical dynamical system

Figure 6: A) The power law for sandpiles. The logarithm of the frequency is linear on the logarithm of the avalanche size, except near the right where the avalanches have bigger size than the half of the system. $\Omega = [0, 100]^2$, initially filled with 3 grains everywhere, followed by 10^6 dropped grains. B) The power-law for the Tropical (piece-wise linear, continuous) dynamical system. In this computer experiment Ω has a side of 1000 units and we throw at random a set P of 10000 points (a random large genotype) using two super-computer clusters.

Work in progress: SOC in "Topological Quantum Gravity" (with R. López Vázquez)

- The dichotomy between continuous and discrete models of our paper (already appearing in the biological models of Turing) has an analogue in topological string theory.
- Iqbar-Vafa-Nekrasov-Okunkov have argued that, when we *"probe space-time beyond the scale α' and going below Planck's scale"*, the *"resulting fluctuations of space time"* can be computed with a classical cellular automaton (a melting crystal) representing *quantum gravitational foam*.
- Their theory is a three-tier system whose levels are respectively classical geometry (Kähler gravity), tropical geometry (toric manifolds) and cellular automata (a discrete melting crystal).

Work in progress: SOC in "Quantum Gravity" (with R. López Vázquez)

The theory described above is also a three-tier system whose levels are classical complex algebraic geometry, tropical geometry (analytic tropical curves) and cellular automata (sandpiles). This seems to be not a coincidence and suggests connections between our model for SOC and their model for quantum gravitational foam.

Work in progress: SOC in "Quantum Gravity" (with R. López Vázquez)

We have progressed bt proving so far that, at the level of partition functions:

$$Z_{\mathrm{Sandpile}} = Z_{\mathrm{IVNO}},$$

by using the Temperley bijection for the dual graph, and ONLY for the hexagonal tiling.

(DETAILS: My 2nd talk next week)